

# Comparison of the Total-Dose and 60 MeV Proton-Irradiation Response of CMOS Transistors Operated at 4.2 K

E. Simoen<sup>1</sup>, C. Claeys<sup>1,2</sup>, *Senior Member, IEEE* and A. Mohammadzadeh<sup>3</sup>

<sup>1</sup>IMEC, Kapeldreef 75, B-3001 Leuven, Belgium

<sup>2</sup>also at KU Leuven, E.E. Dept., Kardinaal Mercierlaan 94, B-3001 Leuven, Belgium

<sup>3</sup>ESTEC, Keplerlaan 1, Noordwijk, The Netherlands

## Abstract

This work describes the response of CMOS transistors fabricated in a 0.7  $\mu\text{m}$  technology, which is adapted for cryogenic applications. The impact on the 4.2 K characteristics of total-dose  $\gamma$ -irradiation up to 100 krad is compared with exposure to 60 MeV protons in the fluence range  $3 \times 10^{10} - 10^{12} \text{ cm}^{-2}$ . Transistor arrays from different processing splits have been compared, in order to study the impact of Lowly Doped Drains (LDDs), a threshold voltage adjust implantation or a p-well on the cryogenic characteristics before and after the irradiation.

Overall, it can be concluded that the technology shows sufficient hardness for the envisaged space mission. The observed radiation-induced changes in the main static device and circuit parameters are typically within a few per cent of the starting value, guaranteeing successful operation for the expected duration. Nevertheless, a few interesting observations have been made, concerning unusual radiation behaviour of the CMOS transistors, which will be highlighted here. For the n-channel devices, a reduction of the 4.2 K drain current kink is reported, while the p-channel transistors show a rebound behaviour in the linear characteristics, after low to moderate proton fluences.

## I. INTRODUCTION

When developing cryogenic read-out electronics for focal-plane arrays, one has to consider the space radiation environment. In the literature, little information can be found regarding the radiation response of microelectronic devices and circuits, especially for the liquid helium temperature (LHT) range [1]-[2]. Furthermore, different effects have to be included, like total-dose response, the impact of displacement damage, transient and single event upsets, etc. [1].

The technology of choice for LHT circuitry is clearly CMOS, as the current gain of bipolar transistors is normally very small at 4.2 K [3]. However, one should take into account the particular device behaviour at these temperatures, as they suffer from carrier freeze-out and related transient and kink effects [4]-[8]. All this indicates that the problem of radiation hardness of cryogenic electronics is a complex interplay between technology, design and operation conditions [1].

In this work, initial results are reported concerning the radiation response of transistors and prototype circuits intended for ESA's Far-InfraRed Space Telescope (FIRST) mission. Beside hardening aspects, the aim was to learn more about the fundamental radiation damage mechanisms at 4.2 K.

## II. EXPERIMENTAL

Test structures and prototype circuits have been fabricated in a 0.7  $\mu\text{m}$  CMOS technology at ALCATEL Microelectronics. Different split batches were processed in order to optimise the LHT circuit behaviour. Particular interest points were the presence of a Lowly Doped Drain (LDD), of a p-well or of a threshold voltage ( $V_T$ ) adjust implantation. The main splits studied have been summarised in Table 1. Transistors with different layout, i.e regular versus closed geometry devices, have been compared both before and after irradiation.

Table 1  
Processing splits of the 0.7  $\mu\text{m}$  cryo-CMOS technology.

Wafer	p-well	$V_T$ adjust	LDD
1	yes	yes	yes
6	yes	yes	
9	yes		yes
11	yes		
13		yes	yes
16		yes	
19			yes
22			

Proton (60 MeV) and <sup>60</sup>Co gamma irradiations (dose rate 5 krad/hour) were both performed at Louvain-la-Neuve, up to a fluence  $\Phi$  between  $3 \times 10^{10}$  and  $10^{12} \text{ cm}^{-2}$  and total-dose of 50 and 100 krad(Si), respectively. These should be more than representative values for the total duration of the FIRST mission. A gate bias ( $V_{gs}$ ) of +5 V was applied to the n-MOSFETs and 0 V to the p-channel devices; all other terminals were grounded during the room temperature exposure.

Post irradiation testing has been performed within 24 to 48 hours, in order to reduce annealing effects as much as

possible. For LHT characterisation, the dual-in-line packaged devices have been mounted on a probe, which was inserted in a liquid helium tank. Input ( $I_d$ - $V_{gs}$ ) measurements at small drain bias  $V_{ds}$  were executed in order to extract the threshold voltage, the subthreshold slope and the transconductance  $g_m$ . Output curves ( $I_d$ - $V_{ds}$ ) yielded information on the kink and hysteresis behaviour typical for 4.2 K operation.

### III. RESULTS AND DISCUSSION

#### A. Linear Characteristics

In this section, the impact of both  $\gamma$ - and proton irradiations on the input characteristics at 4.2 K is described. First, the behaviour in linear operation of the n-MOSFETs is summarised, followed by the results for their p-channel counterparts. As shown elsewhere in more detail, the pre-rad characteristics for the different processing splits of Table 1 can exhibit strong differences in  $V_T$ , maximum transconductance  $g_{mmax}$  and subthreshold swing  $S$  [9]. Here, the focus is on the post-radiation behaviour. The important results will be illustrated mainly for the standard 0.7  $\mu\text{m}$  technology with LDDs (wafer 1) and for its non-LDD counterpart (wafer 6), unless otherwise mentioned. The applied drain voltage  $V_{ds}$  is 25 mV for the n- and -100 mV for most of the irradiated p-channel devices, respectively.

##### 1) n-MOSFETs

The 4.2 K input curves of a gamma irradiated standard-split 10  $\mu\text{m}$ x5  $\mu\text{m}$  n-MOSFET with and without LDDs is shown in Figs 1 and 2, respectively. As expected, the  $V_T$  reduces and the device transconductance in Figs 3 and 4 increases with total-dose, pointing to a build-up of positive charge in the gate oxide or at the interface. Occasionally, a hump in the subthreshold characteristic has been observed, indicative of a parallel conduction path along the LOCOS edges of the device (Fig. 1). However, comparing Figs 1 and 2, it is obvious that the total-dose response depends significantly on the processing split. There is also a marked impact of the device geometry, whereby closed transistors show a better total-dose tolerance. Overall, non-LDD devices (Fig. 2) show better post irradiation performance and are therefore recommended as radiation hard(er).

The superior performance of the non-LDD devices is more clearly illustrated by considering the transconductance in Figs 3 and 4.

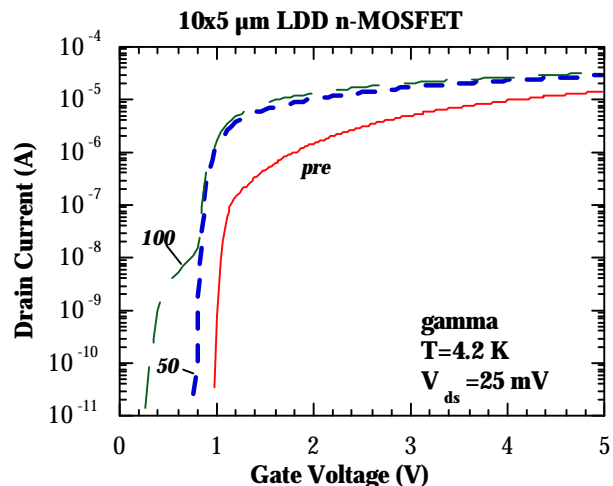


Fig. 1. Input curves at 4.2 K and  $V_{ds}=25$  mV for a 10x5  $\mu\text{m}$  n-MOSFET with LDDs, corresponding to: unirradiated (pre); 50 and 100 krad(Si).

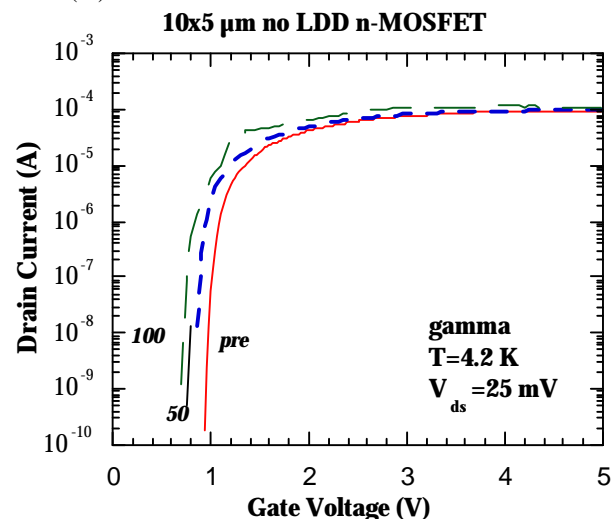


Fig. 2. Input curves at 4.2 K and  $V_{ds}=25$  mV for a 10x5  $\mu\text{m}$  n-MOSFET without LDDs, corresponding to: unirradiated (pre); 50 and 100 krad(Si).

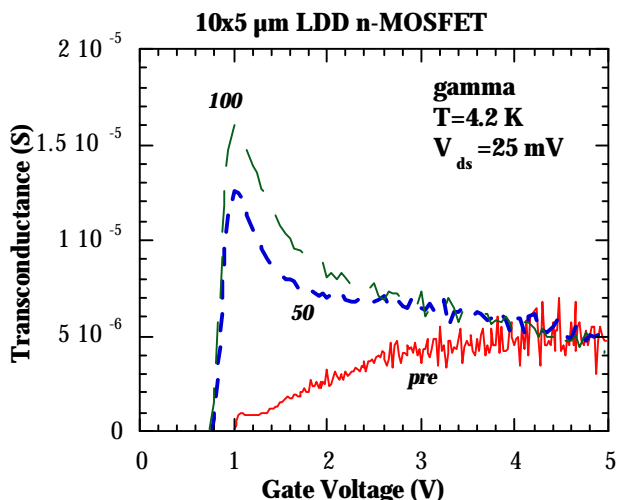


Fig. 3. Transconductance at 4.2 K and  $V_{ds}=25$  mV for a 10x5  $\mu\text{m}$  n-MOSFET with LDDs, corresponding to: unirradiated (pre); 50 and 100 krad(Si).

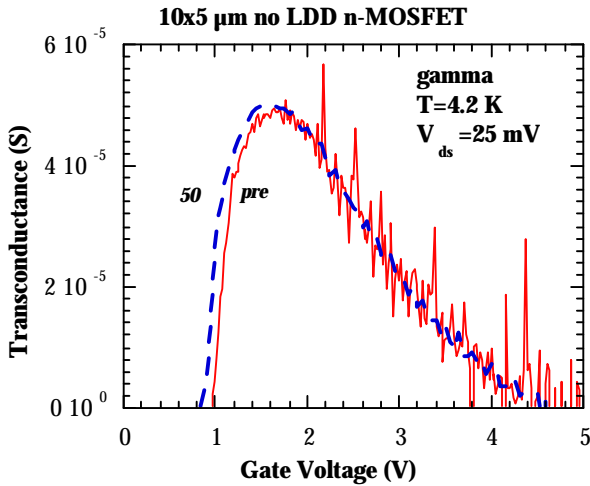


Fig. 4. Transconductance at 4.2 K and  $V_{ds}=25$  mV for a  $10 \times 5$   $\mu\text{m}$  n-MOSFET without LDDs, corresponding to: unirradiated (pre) and 50 krad(Si).

Especially before irradiation, the  $g_m$  of the LDD MOSFETs suffers from insufficient gate-source overlap at small  $V_{ds}$ , which generates a kind of  $V_{ds}$  threshold behaviour [10] and an increase of the series resistance [11]. This results in a rather flat transconductance before irradiation, which contrasts with the peaked behaviour for the non-LDD n-MOSFETs (Fig. 4). After exposure, a peak-shaped transconductance is often observed for the LDD case as well (Fig. 3), pointing to a lowering of the series resistance. The latter is related to the positive oxide-trapping in the spacer oxides above the LDD regions [2].

Qualitatively similar results have been obtained after 60 MeV proton irradiations, as illustrated by Figs 5 to 8. In other words, the n-MOSFETs after exposure show a reduction of the  $V_T$  which increases with fluence  $\Phi$ , while the post-rad transconductance increases (Figs 7 and 8). The increase is most pronounced for the LDD transistors.

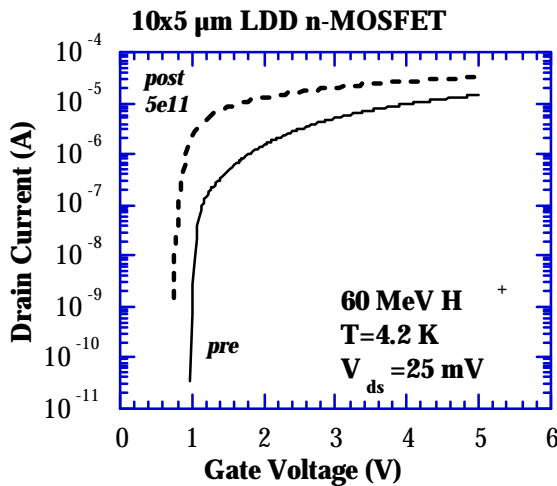


Fig. 5. Input curves at 4.2 K and  $V_{ds}=25$  mV for a  $10 \times 5$   $\mu\text{m}$  n-MOSFET with LDDs, corresponding to: unirradiated (pre) and post a 60 MeV  $5 \times 10^{11}$   $\text{cm}^{-2}$  proton irradiation.

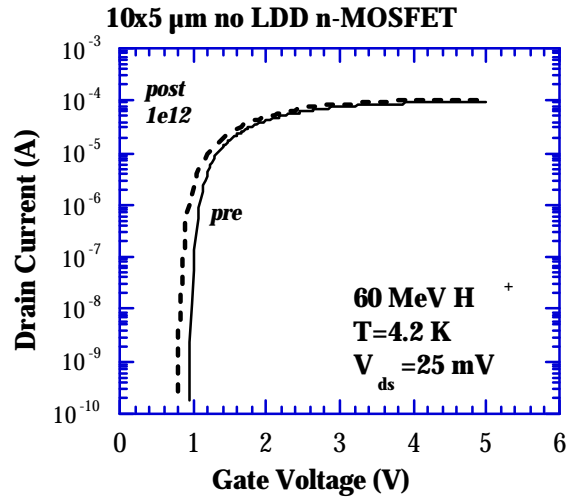


Fig. 6. Input curves at 4.2 K and  $V_{ds}=25$  mV for a  $10 \times 5$   $\mu\text{m}$  n-MOSFET without LDDs, corresponding to: unirradiated (pre) and post a 60 MeV  $10^{12}$   $\text{cm}^{-2}$  proton irradiation.

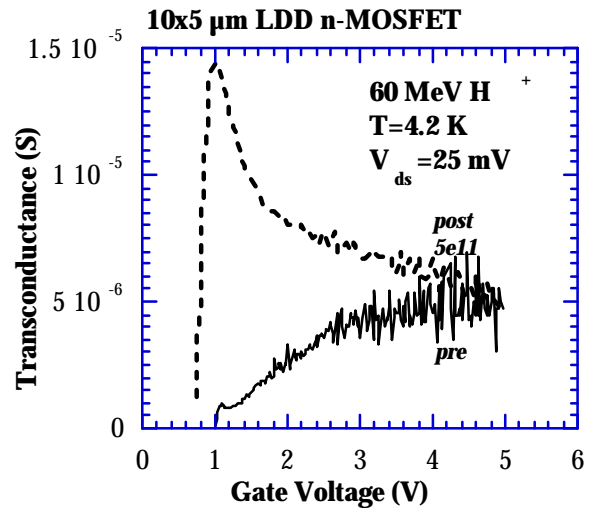


Fig. 7. Transconductance at 4.2 K and  $V_{ds}=25$  mV for a  $10 \times 5$   $\mu\text{m}$  n-MOSFET with LDDs, corresponding to: unirradiated (pre) and post a 60 MeV  $5 \times 10^{11}$   $\text{cm}^{-2}$  proton irradiation.

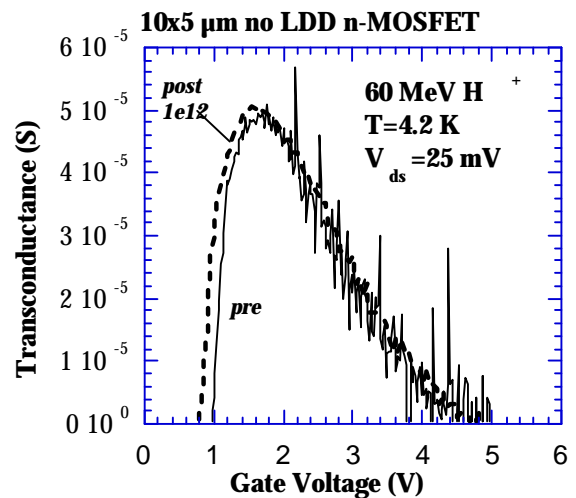


Fig. 8. Transconductance at 4.2 K and  $V_{ds}=25$  mV for a  $10 \times 5$   $\mu\text{m}$  n-MOSFET without LDDs, corresponding to: unirradiated (pre) and post a  $60$  MeV  $10^{12} \text{ cm}^{-2}$  proton irradiation.

## 2) p-MOSFETs

The impact of total-dose on the linear characteristics of the p-MOSFETs at 4.2 K is illustrated in Figs 9 to 12. In this case, a slight reduction of the  $V_T$  towards more negative values is observed, both for LDD (Fig. 9) and non-LDD devices (Fig. 10). The shift becomes more pronounced for a larger total-dose. This is accompanied by a reduction of the transconductance in Fig. 11, while hardly any change is observed in Fig. 12 (non-LDD).

The effects of 60 MeV protons are slightly different, as can be inferred from the results of Fig. 13 and 14, obtained for the non-LDD p-MOSFETs. In this case, the input curve is first shifted to more positive gate voltages for low-to-moderate fluences. After longer exposures, the expected shift is observed.

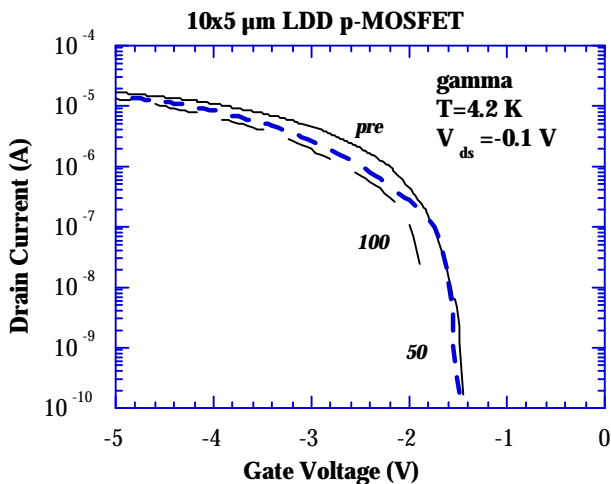


Fig. 9. Input curves at 4.2 K and  $V_{ds}=-0.1$  V for a  $10 \times 5$   $\mu\text{m}$  p-MOSFET with LDDs, corresponding to: unirradiated (pre); 50 and 100 krad(Si).

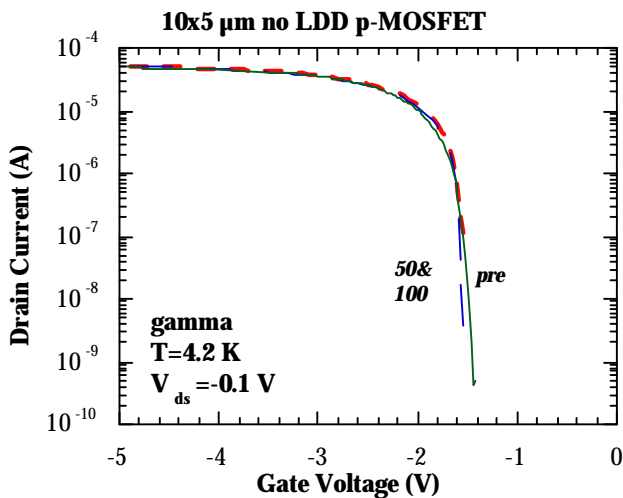


Fig. 10. Input curves at 4.2 K and  $V_{ds}=-0.1$  V for a  $10 \times 5$   $\mu\text{m}$  p-MOSFET without LDDs, corresponding to: unirradiated (pre); 50 and 100 krad(Si).

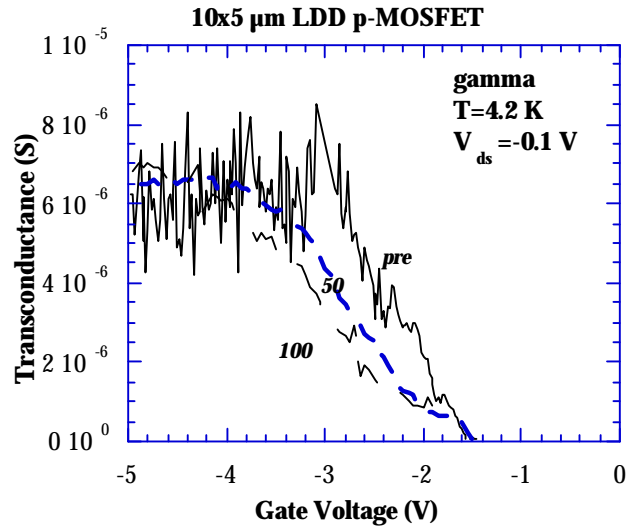


Fig. 11. Transconductance at 4.2 K and  $V_{ds}=-0.1$  V for a  $10 \times 5$   $\mu\text{m}$  p-MOSFET with LDDs, corresponding to: unirradiated (pre); 50 and 100 krad(Si).

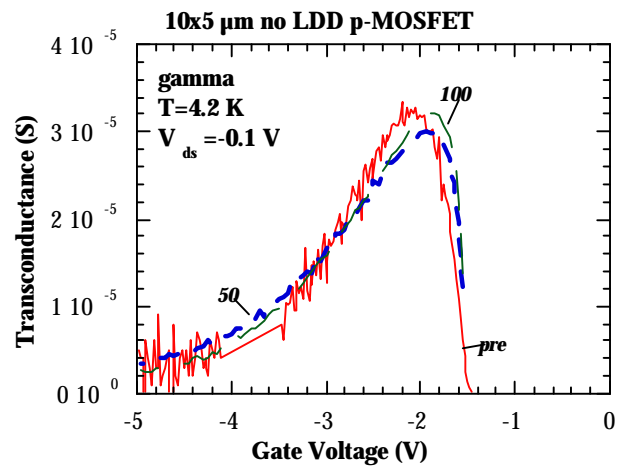


Fig. 12. Transconductance at 4.2 K and  $V_{ds}=-0.1$  V for a  $10 \times 5$   $\mu\text{m}$  p-MOSFET without LDDs, corresponding to: unirradiated (pre); 50 and 100 krad(Si).

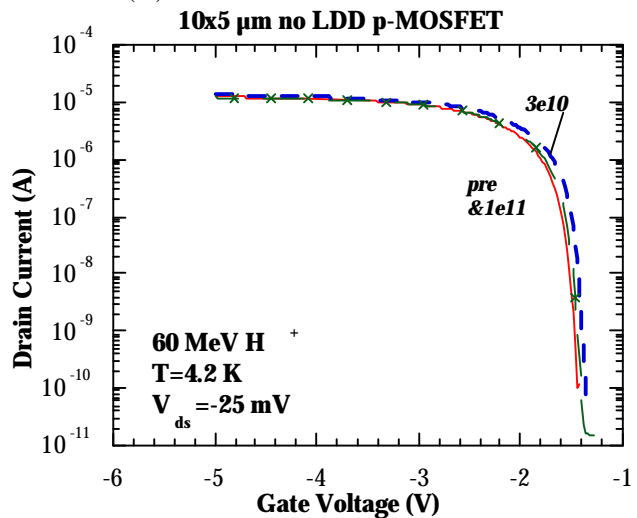


Fig. 13. Input curves at 4.2 K and  $V_{ds}=-25$  mV for a  $10 \times 5$   $\mu\text{m}$  p-MOSFET without LDDs, corresponding to: unirradiated (pre);  $3 \times$  and  $10 \times 10^{10}$   $\text{cm}^{-2}$  60 MeV protons.

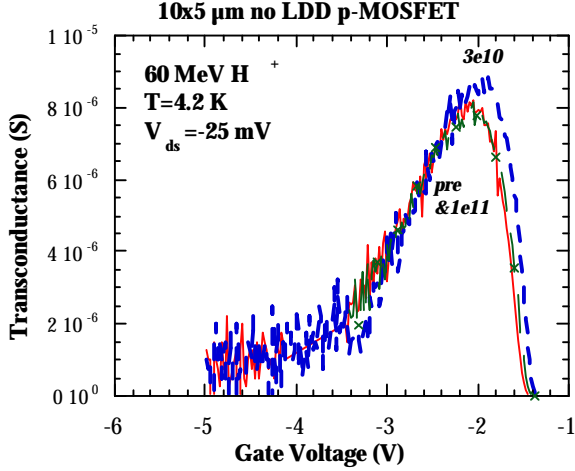


Fig. 14. Transconductance at 4.2 K and  $V_{ds}=-25$  mV for a  $10 \times 5$   $\mu\text{m}$  p-MOSFET without LDDs, corresponding to: unirradiated (pre) an  $3 \times$  and  $10 \times 10^{10}$   $\text{cm}^{-2}$  60 MeV protons.

### 3) Summary

Briefly summarised, it has been observed that after irradiation with  $\gamma$ 's or protons, the  $V_T$  of the n-MOSFETs reduces slightly, while it increases for the p-MOSFETs. This is in line with the expected positive charge trapping in the gate oxide. From the data obtained for the proton irradiated samples in a broad fluence range, it has been found that the reduction of  $V_T$  for the n-MOSFETs can in first instance be modeled by a linear fit, according to [9]:

$$\Delta V_T = -A \Phi \quad (1)$$

with A equal to  $20 \text{ mV}/[10^{10} \text{ protons}/\text{cm}^2]$  for the wafer 1 LDD transistors. For the non-LDD devices of wafer 6, a 20 times lower value has been observed, demonstrating the higher radiation resistance. It is believed that the absence of the inferior quality spacer oxides drastically improves the degradation behaviour [2].

The threshold voltage behaviour of the p-MOSFETs is somewhat more complex, especially for the proton exposures and non-LDD transistors, as demonstrated in Fig. 13. In that case, the  $V_T$  shows an initial increase to more positive values versus fluence, before it drops below its initial value at higher  $\Phi$ . This rebound behaviour is at the moment not quite understood, but it is not unlikely that the room temperature annealing of the radiation damage can play a role in this so-called rebound or ordering effect. Similar improvements in the device performance, after irradiation and anneal have been noted for GaAs and related compounds as well [12]-[13].

Finally, qualitatively similar effects have been found for the change in the transconductance, i.e., a (slight) increase

for n- and a (slight) reduction for the p-channel devices. For proton exposures of the non-LDD devices, a rebound of  $g_m$  is observed as well (Fig. 14). It should be remarked, however, that the LDD devices (both n and p) show a typical behaviour before irradiation, where insufficient gate-source overlap smoothens out the transconductance as a function of the gate voltage. After exposures of LDD transistors, quite often a more regular transconductance peak is observed in Fig. 7, which matches more closely the non-LDD behaviour. Overall, it is concluded that the non-LDD splits are to be preferred for LHT operation both before and after irradiation.

## B. Output Characteristics

### 1) n-MOSFETs

Regarding the output characteristics of the n-channel devices, some interesting behaviour can be noted in Figs 15 and 16. Comparing the pre radiation curves, it is clear that the LDDs play their role in reducing the drain current ( $I_d$ ) kink. However, after  $\gamma$ -exposure, in both cases, little kink is found in the n-channel characteristics. As the kink effect induces circuit non-linearities, a reduction of it after irradiation can be considered an improvement.

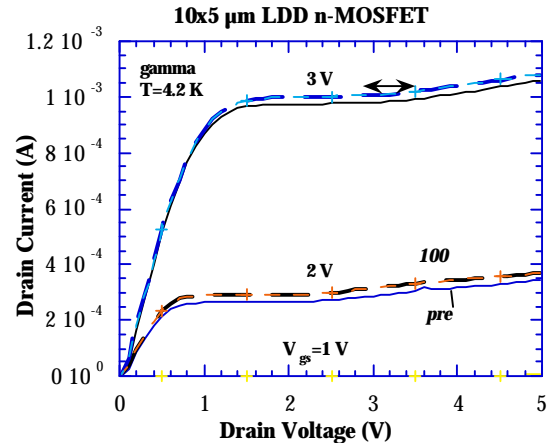


Fig. 15. Output curves at 4.2 K and  $V_{gs}=1,2$  or  $3$  V for a  $10 \times 5$   $\mu\text{m}$  n-MOSFET with LDDs, corresponding to: unirradiated (pre) and 100 krad(Si) (dashes: low-to-high; + high-to-low). No hysteresis is seen, as indicated by the arrow in the upper characteristic.

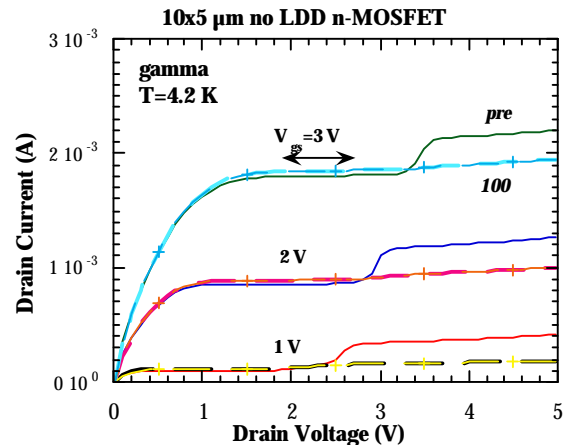


Fig. 16. Output curves at 4.2 K and  $V_{gs}=1,2$  or 3 V for a  $10 \times 5 \mu\text{m}$  n-MOSFET without LDDs (split wafer 11), corresponding to: unirradiated (pre) and 100 krad(Si) (dashes: low-to-high; + high-to-low). No hysteresis is seen, as indicated by the arrow in the upper characteristic.

Similar behaviour is found in Figs 17 (LDD) and 18 (non-LDD) after proton exposures. At the same time, little hysteresis is noted in the output characteristics of Figs 15 to 18, for sufficiently large gate and drain bias.

### 2) p-MOSFETs

The p-MOSFETs show a more pronounced reduction of the drain current in saturation after gamma irradiation (Figs 19 and 20). The changes induced by proton irradiation are analogous, whereby the rebound behaviour is less clear for larger  $V_{ds}$  [9].

### 3) Summary

The 4.2 K output characteristics of the n-MOSFETs are only marginally affected, particularly after the proton irradiations. The saturation current of the p-channel devices, on the other hand, shows a pronounced reduction, which tends to be higher for the LDD splits. Little hysteresis is found for sufficiently high gate and drain bias, both before and after irradiation. For n-MOSFETs without LDDs, a clear drain current kink has been found. However, after irradiation and irrespective of the projectile, a reduction of the kink effect at 4.2 K is noted. This is ascribed to the lower multiplication rate, as will be reported in a forthcoming publication [14].

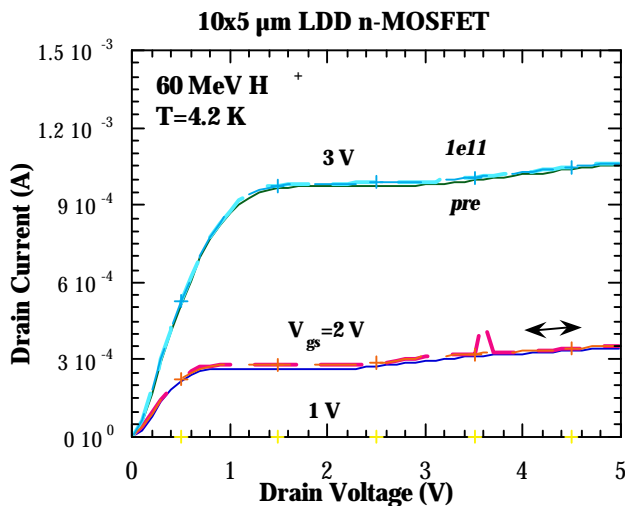


Fig. 17. Output curves at 4.2 K and  $V_{gs}=1,2$  or 3 V for a  $10 \times 5 \mu\text{m}$  n-MOSFET with LDDs, corresponding to: unirradiated (pre) and  $10^{11} \text{cm}^{-2}$  proton irradiated (dashes: low-to-high; + high-to-low). No hysteresis is seen, as indicated by the arrow in the lower characteristic.

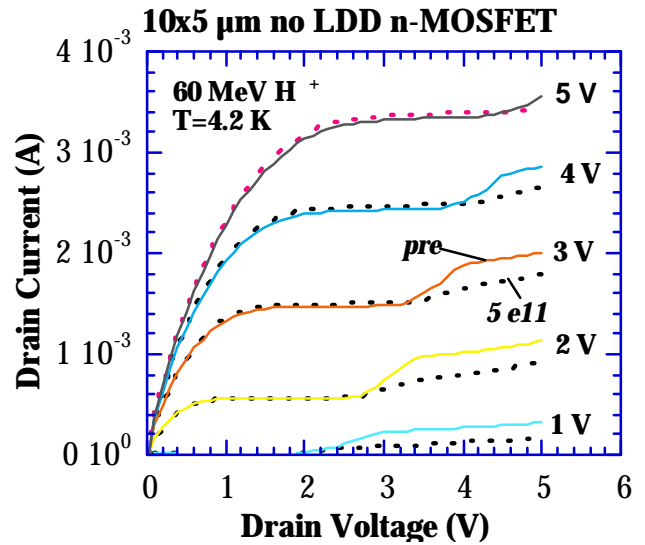


Fig. 18. Output curves at 4.2 K and  $V_{gs}=1$  to 5 V for a  $10 \times 5 \mu\text{m}$  n-MOSFET without LDDs (split #16), corresponding to: unirradiated (pre) and  $5 \times 10^{11} \text{cm}^{-2}$  proton irradiated (dashes).

It should finally be remarked that also read-out electronic circuits fabricated in the  $0.7 \mu\text{m}$  technology have been tested at 4.2 K, before and after irradiation by gammas and protons. The same total-dose and fluence range has been studied. Within the measurement accuracy, no pronounced degradation or malfunctioning has been observed [9], indicating that the technology will fulfill the hardness requirements of the FIRST mission.

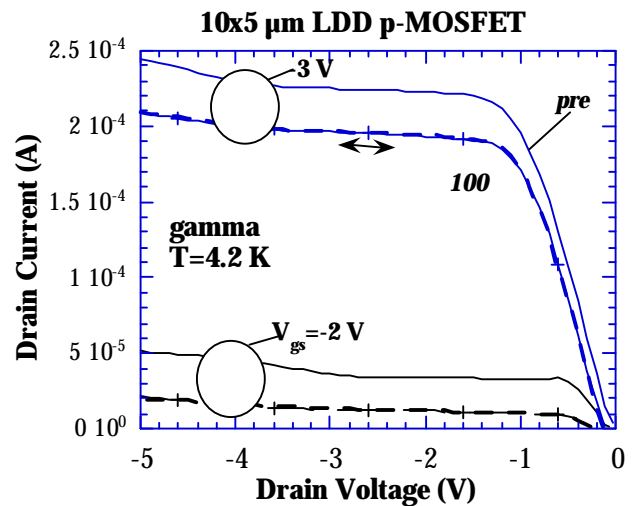


Fig. 19. Output curves at 4.2 K and  $V_{gs}=-2$  or  $-3$  V for a  $10 \times 5 \mu\text{m}$  p-MOSFET with LDDs, corresponding to: unirradiated (pre) and 100 krad(Si) (dashes: high-to-low and +: low-to-high). No hysteresis is seen, as indicated by the arrow in the upper characteristic.

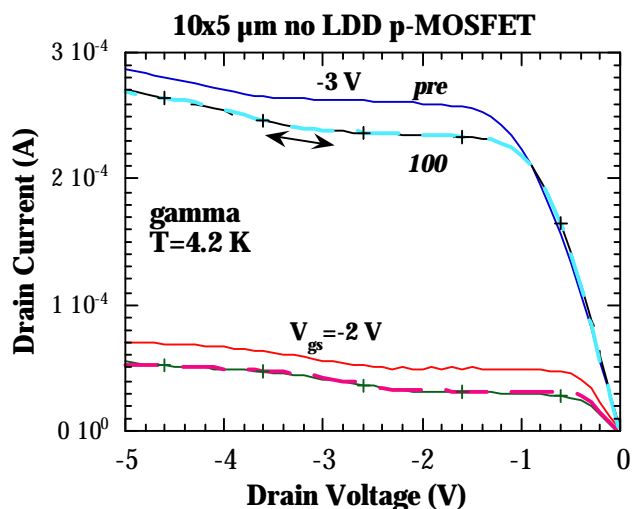


Fig. 20. Output curves at 4.2 K and  $V_{gs} = -2$  or  $-3$  V for a  $10 \times 5 \mu\text{m}$  p-MOSFET with LDDs, corresponding to: unirradiated (pre) and 100 krad(Si) (dashes: high-to-low and +: low-to-high). No hysteresis is seen, as indicated by the arrow in the upper characteristic.

#### IV. CONCLUSIONS

From these initial radiation tests it is first of all concluded that the technology is sufficiently hard for the mission envisaged. Better radiation tolerance is expected for the non LDD splits, without threshold voltage adjust. The occurrence of some low-temperature specific phenomena indicates that additional fundamental radiation mechanisms are operational at cryogenic temperatures, which require further in-depth studies.

#### REFERENCES

- [1] C. Claeys and E. Simoen, "Literature study on radiation effects in cryogenic electronics", Deliverable D1, Work Order 1938/NL/LB, October 1997.
- [2] R.L. Pease, S.D. Clark, P.L. Cole, J.F. Krieg, and J.C. Pickel, "Total dose response of transconductance in MOSFETs at low temperature", *IEEE Trans. Nucl. Sci.*, vol. NS-41, pp. 549-554, June 1994.
- [3] T.S. Jayadev, S. Ichiki, and J.C.S. Woo, "Bipolar transistors for low noise, low temperature electronics", *Cryogenics*, vol. 30, pp. 137-140, February 1989.
- [4] C.G. Rogers, "MOST's at cryogenic temperatures", *Solid-State Electron.*, vol. 11, p. 1079-1091, Nov. 1968.
- [5] F. Balestra, L. Audaire, and C. Lucas, "Influence of substrate freeze-out on the characteristics of MOS transistors at very low temperatures", *Solid-State Electron.*, vol. 30, pp. 321-327, March 1987.
- [6] B. Dierickx, L. Warmerdam, E. Simoen, J. Vermeiren, and C. Claeys, "Model for hysteresis and kink behavior of MOS transistors operating at 4.2 K", *IEEE Trans. Electron Devices*, vol. ED-35, pp. 1120-1125, July 1988.
- [7] K.L. Kasley, G.M. Oleszek, and R.L. Anderson, "Investigation of the kink and hysteresis from 13 K to 30 K

in n-channel CMOS transistors with a floating well", *Solid-State Electron.*, vol. 36, pp. 945-948, July 1993.

[8] E. Simoen and C. Claeys, "Impact ionization related phenomena in Si MOSFETs operating at cryogenic temperatures", In: *Proc. of the Fourth Symposium on Low Temperature Electronics and High Temperature Superconductivity*, Eds C.L. Claeys, S.I. Raider, M.J. Deen, W.D. Brown and R.K. Kirschman, The Electrochem. Soc. Proc. Vol. 97-2, The Electrochem. Soc. (Pennington, NJ), pp. 117-139, 1997.

[9] C. Claeys and E. Simoen, "Radiation testing of cryogenic devices and circuits", Deliverable D2, Work Order 1938/96/NL/LB, February 1999.

[10] E.A. Gutiérrez D., "The drain threshold voltage  $V_{T_D}$  in submicrometer MOS transistors at 4.2 K", *IEEE Electron Device Lett.*, vol. 16, pp. 85-87, March 1995.

[11] I.M. Hafez, G. Ghibaudo, F. Balestra, and M. Haond, "Impact of LDD structures on the operation of silicon MOSFETs at low temperature", *Solid-State Electron.*, vol. 38, pp. 419-424, February 1995.

[12] S.M. Khanna, C. Rejeb, A. Jorio, M. Parenteau, C. Carlone, and J.W. Gerdes, Jr., "Electron and neutron radiation-induced order effect in gallium arsenide", *IEEE Trans. Nucl. Sci.*, vol. NS-40, pp. 1350-1359, December 1993.

[13] A. Jorio, M. Parenteau, M. Aubin, C. Carlone, S.M. Khanna, and J.W. Gerdes, Jr., "A mobility study of the radiation induced order effect in gallium arsenide", *IEEE Trans. Nucl. Sci.*, vol. NS-41, pp. 1937-1944, December 1994.

[14] E. Simoen, C. Claeys, and A. Mohammadzadeh, "Impact of ionising irradiation on the drain current kink at 4.2 K in cryogenic n-MOSFETs", Paper submitted for publication in *IEEE Electron Device Lett.*

